

Semi-Supervised Semantic Segmentation with Pixel-Level Contrastive Learning from a Class-wise Memory Bank

Inigo Alonso
University of Zaragoza
inigo@unizar.es

Alberto Sabater
University of Zaragoza
asabater@unizar.es

David Ferstl
Magic Leap
dferstl@magicleap.com

Luis Montesano
University of Zaragoza
montesano@unizar.es

Ana C. Murillo
University of Zaragoza
acm@unizar.es

Abstract

This work presents a novel approach for semi-supervised semantic segmentation, i.e., per-pixel classification problem assuming that only a small set of the available data is labeled. We propose a novel representation learning module based on contrastive learning. This module enforces the segmentation network to yield similar pixel-level feature representations for same-class samples across the whole dataset. To achieve this, we maintain a memory bank continuously updated with feature vectors from labeled data. These features are selected based on their quality and relevance for the contrastive learning. In an end-to-end training, the features from both labeled and unlabeled data are optimized to be similar to same-class samples from the memory bank. Our approach outperforms the current state-of-the-art for semi-supervised semantic segmentation and semi-supervised domain adaptation on well-known public benchmarks, with larger improvements on the most challenging scenarios, i.e., less available labeled data.

1. Introduction

The goal of semantic segmentation consists in assigning a semantic class label to each pixel in an image. It is an essential computer vision task for semantic scene understanding that plays a relevant role in many applications such as medical imaging [31] or autonomous driving [2].

As for many other computer vision tasks, deep convolutional neural networks have shown significant improvements in semantic segmentation [2, 21, 1]. All these examples follow supervised learning approaches, which require a large set of annotated data to be able to generalize well. However, the availability of labeled data is a common bottleneck in supervised learning, especially for tasks such as

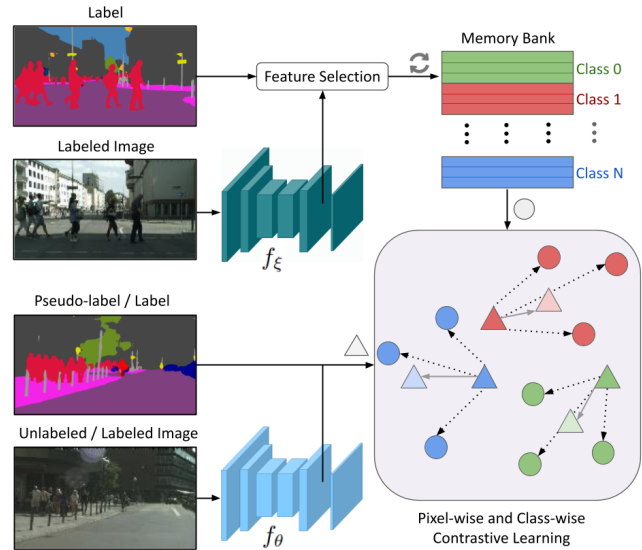


Figure 1. **Proposed contrastive learning module overview.** At each training iteration, the teacher network f_ξ updates the feature memory bank with a subset of selected features from labeled samples. Then, the student network f_θ extracts features Δ from both labeled and unlabeled samples, which are optimized to be similar to same-class features from the memory bank \bigcirc .

semantic segmentation, which require tedious and expensive per-pixel annotations.

Semi-supervised learning assumes that only a small subset of the available data is labeled. It tackles this limited labeled data issue by extracting knowledge from unlabeled samples. Semi-supervised learning has been applied to a wide range of applications [38], including semantic segmentation [13, 19, 27]. Previous semi-supervised segmentation works are mostly based on per-sample entropy minimization [19, 23, 29] and per-sample consistency regularization [13, 37, 29]. These segmentation methods do not

enforce any type of structure on the learned features to increase inter-class separability across the whole dataset.

Our hypothesis is that overcoming this limitation can lead to better feature learning. In particular, we expect to learn better from the unlabeled data, which is critical when the amount of available labeled data is low.

This work presents a novel approach for semi-supervised semantic segmentation. Our approach follows a teacher-student scheme whose main component is a novel representation learning module (see Figure 1). This module is based on contrastive learning [17] and enforces the class-separability of pixel-level features. To achieve this, the teacher network produces feature candidates, only from labeled data, to be stored in a memory bank. Meanwhile, the student network learns to produce similar class-wise features from both labeled and unlabeled data. The features introduced in the memory bank are selected based on their quality and on their learned relevance for the contrastive optimization. In addition to increased inter-class separability, the module enforces the alignment of unlabeled and labeled data (memory bank) in the feature space, which is another unexploited idea in semi-supervised semantic segmentation.

The effectiveness of the proposed approach is demonstrated on well-known benchmarks for semi-supervised semantic segmentation, reaching the state-of-the-art on different set-ups. Additionally, our approach can naturally tackle the semi-supervised domain adaptation task, also obtaining state-of-the-art results. In all cases, the improvements upon comparable methods increase with the percentage of unlabeled data. The detailed ablation study performed shows the significance of the different components of the proposed approach. Code is available as supplementary material and will be made publicly available upon acceptance.

2. Related Work

This section summarizes relevant related work for contrastive learning and semi-supervised learning, with particular emphasis on work related to semantic segmentation.

2.1. Contrastive Learning.

The core idea of contrastive learning [17] is to create positive and negative pairs from data, to attract the positive and repulse the negative pairs in the feature space. However, recent works [7, 16, 18] have shown similar level of performance using positive pairs only. The main difference in current methods is how to obtain these pairs: by using a memory bank [43], by using a momentum model [6] or directly from the same batch [5]. Contrastive learning has been recently popularized for self-supervised representation learning [6, 16, 43, 46]. As for semantic segmentation, contrastive learning has been mainly used as pre-training [41, 44, 45]. Very recently, Wang *et al.* [40] have

shown improvements in supervised scenarios applying contrastive learning in a pixel and region level for same-class supervised samples. Van *et al.* [39] have shown the advantages of contrastive learning in unsupervised set-ups, applying it between features from different saliency masks.

In this work, we propose to use contrastive learning to boost the performance in semi-supervised semantic segmentation tasks. Differently from previous works, our contrastive module aligns features from both labeled and unlabeled data to high-quality features from all over the labeled set that are stored in a memory bank. We follow the positive-only research branch for computational efficiency.

2.2. Semi-Supervised Learning

This section discusses the two most common strategies for semi-supervised learning, pseudo-labeling and consistency regularization, as well as the application of semi-supervised learning to semantic segmentation.

Pseudo-Labeling. Pseudo-labeling leverages the idea of creating artificial labels for unlabeled data [25, 33] by keeping the most likely predicted class by an existing model [23]. The use of pseudo-labels is motivated by entropy minimization [15], encouraging the network to output highly confident probabilities on unlabeled data. Both pseudo-labeling and direct entropy minimization methods are commonly used in semi-supervised scenarios [11, 22, 34, 29] showing great performance. Our approach makes use of both pseudo-labels and direct entropy minimization.

Consistency Regularization. Consistency regularization relies on the assumption that the model should be invariant to perturbations, *e.g.*, data augmentation, made to the same image. This regularization is commonly applied by using two different methods: distribution alignment [3, 32, 36], or augmentation anchoring [34]. While the distribution alignment enforces the predicted class distributions of perturbed images to be the same as the non-perturbed image class distribution, the augmentation anchoring forces the perturbed images to be classified as the non-perturbed image. While distribution alignment enforces the perturbed and non-perturbed to have the same class distribution, augmentation anchoring enforces them to have the same semantic label. To produce high-quality non-perturbed class distribution or prediction on unlabeled data, the Mean Teacher method [37], proposes a teacher-student scheme where the teacher network is an exponential moving average (EMA) of model parameters, producing more robust predictions.

In this work, we apply the anchoring augmentation strategy and use an EMA model for computing the pseudo-labels.

2.3. Semi-Supervised Semantic Segmentation.

Semi-supervised learning addresses the problem of the high annotation cost by assuming that only a small subset of the available data is labeled, while the rest remains unlabeled. One common approach for this task is to make use of Generative Adversarial Networks (GANs) [14]. Hung *et al.* [19] propose to train the discriminator to distinguish between confidence maps from labeled and unlabeled data predictions. Mittal *et al.* [27] make use of a two-branch approach, one branch enforcing low entropy predictions using a GAN approach and another branch for removing false-positive predictions using a Mean Teacher method [36]. A similar idea was proposed by Feng *et al.* [12], a recent work that introduces Dynamic Mutual Training (DMT). DMT uses two segmentation models and the model’s disagreement is used to re-weight the loss. DMT method also followed the multi-stage training protocol from CBC [11], where pseudo-labels are generated in an offline curriculum fashion. Other works are based on data augmentation methods for consistency regularization. French *et al.* [13] focus on applying CutOut [9] and CutMix [47], while Olsson *et al.* [29] propose a data augmentation technique specific for semantic segmentation.

Differently from previous work, we propose a novel feature learning module that shows the benefits of incorporating consistent learning in a semi-supervised scenario.

3. Method

Semi-supervised semantic segmentation consists in a per-pixel classification task where two different sources of data are available: a few fully-labeled samples $\mathcal{X}_l = \{x_l, y_l\}$, where x_l are the training images and y_l their corresponding per-pixel annotations, and a large set of unlabeled samples $\mathcal{X}_u = \{x_u\}$.

To tackle this task, we propose to use a teacher-student scheme. The teacher network f_ξ creates robust pseudo-labels from unlabeled samples and memory bank entries from labeled samples to teach the student network f_θ to improve its segmentation performance.

Teacher-student scheme. The learned weights θ of the student network f_θ are optimized using the following loss function:

$$\mathcal{L} = \lambda_{sup} \mathcal{L}_{sup} + \lambda_{pseudo} \mathcal{L}_{pseudo} + \lambda_{ent} \mathcal{L}_{ent} + \lambda_{contr} \mathcal{L}_{contr}. \quad (1)$$

The \mathcal{L}_{sup} is the loss for supervised learning on labeled samples (Section 3.1). \mathcal{L}_{pseudo} and \mathcal{L}_{ent} tackle pseudo-labels (Section 3.2) and entropy minimization (Section 3.3) techniques, respectively, where the pseudo-labels are generated by the teacher segmentation network f_ξ . Finally, \mathcal{L}_{contr} is our proposed contrastive learning loss (Section 3.4).

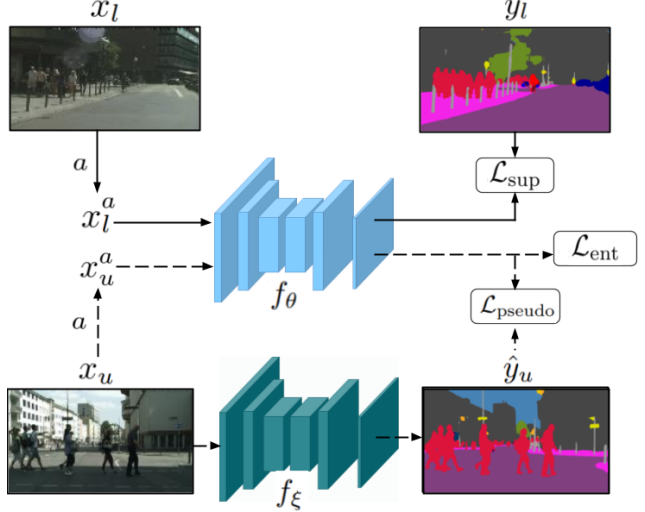


Figure 2. **Supervised and self-supervised optimization.** The student network f_θ is optimized by the supervised loss (\mathcal{L}_{sup}) for labeled data (x_l, y_l) . For unlabeled data x_u , the teacher network f_ξ computes the pseudo-labels \hat{y}_u that are later used for optimizing the pseudo-labels loss (\mathcal{L}_{pseudo}) for pairs of augmented samples and pseudo-labels (x_u^a, \hat{y}_u) . Direct entropy minimization (\mathcal{L}_{ent}) is also applied on predictions from x_u^a .

Weights ξ of the teacher network f_ξ are an exponential moving average of weights θ of the student network f_θ with a decay rate $\tau \in [0, 1]$. The teacher model provides more accurate and robust predictions [37]. Thus, at every training step, the teacher network f_ξ is not optimized by a gradient descent but updated as follows:

$$\xi = \tau \xi + (1 - \tau) \theta. \quad (2)$$

3.1. Supervised Segmentation: \mathcal{L}_{sup}

Our supervised semantic segmentation optimization, applied to the labeled data \mathcal{X}_l , follows the standard optimization with the weighted cross-entropy loss. Let \mathcal{H} be the weighted cross-entropy loss between two lists of N per-pixel class probability distributions y_1, y_2 :

$$\mathcal{H}(y_1, y_2) = -\frac{1}{N} \sum_{n=1}^N \sum_{c=1}^C y_2^{(n,c)} \log(y_1^{(n,c)}) \alpha^c \beta^n, \quad (3)$$

where C is the number of classes to classify, N is the number of elements, *i.e.*, pixels in y_1 , α^c is a per-class weight, and, β^n is a per-pixel weight. Specific values of α^c and β^n are detailed in Section 4.2. The supervised loss (see top part of Figure 2) is defined as follows:

$$\mathcal{L}_{sup} = \mathcal{H}(f_\theta(x_l^a), y_l), \quad (4)$$

where x_l^a is a weak augmentation of x_l (see Section 4.2 for augmentation details).

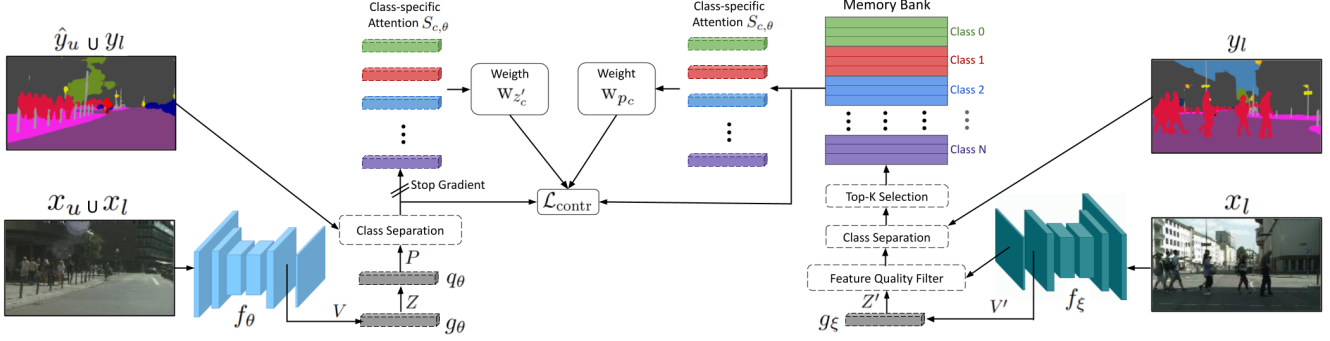


Figure 3. **Contrastive learning optimization.** At every iteration, features are extracted by f_ξ from labeled samples (see right part). These features are projected, filtered by their quality, and then, ranked to finally only store the highest-quality features into the memory bank. Concurrently, feature vectors from input samples extracted by f_θ are fed to the projection and prediction heads (see left part). Then, feature vectors are passed to a self-attention module in a class-wise fashion, getting a per-sample weight. Finally, input feature vectors are enforced to be similar to same-class features from the memory bank.

3.2. Learning from Pseudo-labels: $\mathcal{L}_{\text{pseudo}}$

The key to the success of semi-supervised learning is to learn from unlabeled data. One idea our approach exploits is to learn from pseudo-labels. In our case, pseudo-labels are generated by the teacher network f_ξ (see Figure 2). For every unlabeled sample x_u , the pseudo-labels \hat{y}_u are computed following this equation:

$$\hat{y}_u = \arg \max f_\xi(x_u), \quad (5)$$

where f_ξ predicts a class probability distribution. Note that pseudo-label generation is performed in an online fashion at each training iteration.

Consistency regularization is introduced by using augmentation anchoring, *i.e.*, computing different data augmentation for each sample x_u on the same batch, which helps the model to converge to a better solution [34]. The pseudo-labels loss for unlabeled data \mathcal{X}_u is calculated by the cross-entropy:

$$\mathcal{L}_{\text{pseudo}} = \frac{1}{A} \sum_{a=1}^A \mathcal{H}(f_\theta(x_u^a), \hat{y}_u), \quad (6)$$

where x_u^a is a strong augmentation of x_u and A is the number of augmentations we apply to sample x_u (see Section 4.2 for augmentation details).

3.3. Direct Entropy Minimization: \mathcal{L}_{ent}

Direct entropy minimization is applied on the class distributions predicted by the student network from unlabeled samples x_u as a regularization loss:

$$\mathcal{L}_{\text{ent}} = -\frac{1}{A} \frac{1}{N} \sum_{a=1}^A \sum_{n=1}^N \sum_{c=1}^C f_\theta(x_u^{a,n,c}) \log f_\theta(x_u^{a,n,c}), \quad (7)$$

where C is the number of classes to classify, N is the number of pixels and A is the number of augmentations.

3.4. Contrastive Learning: $\mathcal{L}_{\text{contr}}$

Figure 3 illustrates our proposed contrastive optimization. A memory bank is filled with high-quality feature vectors from the teacher network f_ξ (right part of Figure 3). Concurrently, the student network f_θ extracts feature vectors from either \mathcal{X}_l or \mathcal{X}_u . In a per-class fashion, every feature is passed through a simple self-attention module that serves as per-feature weighting in the contrastive loss. Finally, the contrastive loss enforces the weighted feature vectors from the student to be similar to feature vectors from the memory bank. As the memory bank contains high-quality features from all labeled samples, the contrastive loss helps to create a better class separation in the feature space across the whole dataset as well as aligning the unlabeled data distribution with the labeled data distribution.

Contrastive Learning Optimization. Let $f_{\theta-}$ be the student network without the classification layer and $\{x, y\}$ a training sample that is either from the labeled $\{\mathcal{X}_l, \mathcal{Y}_l\}$ or unlabeled set $\{\mathcal{X}_u, \hat{\mathcal{Y}}_u\}$. The first step is to extract all feature vectors: $V = f_{\theta-}(x)$. The feature vectors V are then fed to a projection head, $Z = g_\theta(V)$, and a prediction head, $P = q_\theta(Z)$, following [16], where g_θ and q_θ are two different Multi-Layer Perceptrons (MLPs). Next, P is grouped by the different semantic classes in y .

Let $P_c = \{p_c\}$ be the set of prediction vectors from P of a specific class c . Let $Z'_c = \{z'_c\}$ be the set of projection vectors of class c obtained by the teacher network, $Z' = g_\xi(f_{\xi-}(x))$ from the labeled examples stored in the memory bank, *i.e.*, memory entries.

Next, we learn which feature vectors (p_c and z'_c) are beneficial for the contrastive learning task, by assigning per-feature learned weights (Equation 8) that will serve as a weighting factor (Equation 10) for the contrastive learning loss function (Equation 11). These per-feature weights are

computed using class-specific attention modules $S_{c,\theta}$ (see Section 4.2 for further details) that generate a single value ($w \in [0, 1]$) for every z'_c and p_c feature. Following [35] we L1 normalize these weights to prevent converging to the trivial all-zeros solution. For the prediction vectors P_c case, the weights w_{p_c} are then computed as follows:

$$w_{p_c} = \frac{|P_c|}{\sum_{p_i \in P_c} S_{c,\theta}(p_i)} S_{c,\theta}(p_c). \quad (8)$$

Equation 8 is also used to compute $w_{z'_c}$, but using Z'_c and z'_c instead of P_c and p'_c .

The contrastive loss is computed to attract prediction vectors p_c to be similar to projection vectors from the memory bank z'_c . For that, we use the cosine similarity as the similarity measure C :

$$C(p_c, z'_c) = \frac{\langle p_c, z'_c \rangle}{\|p_c\|_2 \cdot \|z'_c\|_2}, \quad (9)$$

where, the weighted distance between predictions and memory bank entry is computed by:

$$\mathcal{D}(p_c, z'_c) = w_{p_c} w_{z'_c} (1 - C(p_c, z'_c)), \quad (10)$$

and finally, our contrastive loss is computed as follows:

$$\mathcal{L}_{contr} = \frac{1}{C} \frac{1}{|P_c|} \frac{1}{|Z'_c|} \sum_{c=1}^C \sum_{p_c \in P_c} \sum_{z'_c \in Z'_c} \mathcal{D}(p_c, z'_c). \quad (11)$$

Memory Bank. The memory bank is the data structure that maintains the target feature vectors z'_c, ψ for each class c , used in the contrastive loss. In our case, it contains only high-quality pixel-level feature vectors from labeled data.

As shown in Figure 3, the memory bank is updated on every training iteration with a subset of $z'_c \in Z'$ generated by the teacher network. To select what subset of Z' is included in the memory bank, we first perform a Feature Quality Filter (FQF), where we only keep features that lead to an accurate prediction when the classification layer is applied, $y = \arg \max f_\xi(x_l)$, having confidence higher than a threshold, $f_\xi(x_l) > \phi$. The remaining Z' are grouped by classes Z'_c . Finally, instead of picking randomly a subset of every Z'_c to update the memory bank, we make use of the class-specific attention modules $S_{c,\xi}$. We get ranking scores $R_c = S_{c,\xi}(Z'_c)$ to sort Z'_c and we update the memory bank only with the top-K highest-scoring vectors. The memory bank is a First In First Out (FIFO) queue per class for computation and time efficiency. This way it maintains recent high-quality feature vectors in a very efficient fashion computation-wise and time-wise. Detailed information about the hyper-parameters is included in Section 4.2.

4. Experiments

This section describes the datasets and implementation details used in the evaluation of the presented work. It also contains the comparison of our method with the state-of-the-art on different benchmarks for semi-supervised semantic segmentation, including a semi-supervised domain adaptation set-up, and a detailed ablation study.

4.1. Datasets

- Cityscapes [8]. It is a real urban scene dataset composed of 2975 training and 500 validation samples, with 19 semantic classes.
- PASCAL VOC 2012 [10]. It is a natural scenes dataset with 21 semantic classes. The dataset has 10582 and 1449 images for training and validation respectively.
- GTA5 [30]. It is a synthetic dataset captured from a video game with realistic urban-like scenarios with 24966 images in total. The original dataset provides 33 different categories but, following [42], we only use the 19 classes that are shared with Cityscapes.

4.2. Implementation details

Architecture. We use DeepLab networks [4] in our experiments. For the ablation study and most benchmarking experiments, DeepLabv2 with a ResNet-101 backbone is used for a fair comparison (*i.e.*, similar settings) to previous works [29, 11, 19, 27]. DeepLabv3+ with Resnet50 backbone is also used to equal comparison with [26]. For the teacher network f_ξ , we set $\tau = 0.997$ in (Equation 2).

The prediction and projection heads follow [16]: Linear \rightarrow BatchNorm [20] \rightarrow Relu [28] \rightarrow Linear, with a hidden and output dimension of 256. The proposed class-specific attention modules follow a similar architecture: Linear \rightarrow BatchNorm \rightarrow LeakyRelu [24] \rightarrow Linear \rightarrow Sigmoid, with a hidden and output dimension of 256 and 1 respectively. We use $2 \times N_{classes}$ attention modules since they are used in a class-wise fashion. In particular, two modules per class are used because we have different modules for projection or prediction feature vectors.

Following previous works [29, 37], the segmentation is performed with the student network f_θ in the experimental validation.

Optimization. For all experiments, we train for 80K iterations using the SGD optimizer with a momentum of 0.9. The learning rate is set to 2×10^{-4} for DeepLabv2 and 4×10^{-4} for DeepLabv3+ with a poly learning rate schedule. For the Cityscapes and GTA5 datasets, we use a crop size of 512×512 and batch sizes of 5 and 7 for Deeplabv2 and Deeplabv3+, respectively. For Pascal VOC, we use

a crop size of 321×321 and batch sizes of 14 and 20 for Deeplabv2 and Deeplabv3+, respectively. Cityscapes images are downsampled to 512×1024 before cropping when Deeplabv2 is used for a fair comparison with previous works [29, 11, 19, 27]. The different loss weights in (Equation 1) are set as follows for all experiments: $\lambda_{sup} = 1$, $\lambda_{pseudo} = 1$, $\lambda_{ent} = 0.01$, $\lambda_{contr} = 0.1$. An exception is made for the first 2K training iterations where $\lambda_{contr} = 0$ and $\lambda_{pseudo} = 0$ to make sure predictions have some quality before being taken into account. Regarding the per-pixel weights (β^n) from \mathcal{H} in (Equation 3), we set it to 1 for \mathcal{L}_{sup} . For \mathcal{L}_{pseudo} , we follow [11] weighting each pixel with its corresponding pseudo-label confidence with a sharpening operation, $f_\xi(x_u)^s$, where we set $s = 6$. As for the per-class weights α^c in (Equation 3), we perform a class balancing for the Cityscapes and GTA5 datasets by setting $\alpha^c = \sqrt{\frac{f_m}{f_c}}$ with f_c being the frequency of class c and f_m the median of all class frequencies. In semi-supervised settings the amount of labels, Y_l , is usually small. For the Pascal VOC we set $\alpha^c = 1$ as the class balancing does not have a beneficial effect.

Other details. DeepLab’s output resolution is $\times 8$ lower than the input resolution. For feature comparison during training, we keep the output resolution and downsample the labels reducing memory requirements and computation.

The memory bank size is fixed to $\psi = 256$ vectors per class (see Section 4.4 for more details). The confidence threshold ϕ for accepting features is set to 0.95. The number of vectors added to the memory bank at each iteration, for each image, and for each class is set as $\max(1, \frac{\psi}{|\mathcal{X}_l|})$, where $|\mathcal{X}_l|$ is the number of labeled samples.

A single NVIDIA Tesla V100 GPU is used for all experiments. All our reported results are the mean of three different runs with different labeled/unlabeled data splits.

Data augmentation. In our work, we use two different augmentation set-ups, a weak augmentation for labeled samples and a strong augmentation set-up for unlabeled samples, see Table 1 for configuration details. For the augmentation anchoring (Equation 6), we set $A = 2$ as the number of augmentations for the same sample.

4.3. Benchmark Experiments

The following experiments compare the proposed method with state-of-the-art methods in different semi-supervised semantic segmentation set-ups, including the semi-supervised domain adaptation scenario.

Table 1. Strong and weak data augmentation set-ups

Parameter	Weak	Strong
Flip probability	0.50	0.50
Resize $\times [0.75, 1.75]$ probability	0.50	0.80
Color jittering probability	0.20	0.80
Brightness adjustment max intensity	0.15	0.30
Contrast adjustment max intensity	0.15	0.30
Saturation adjustment max intensity	0.075	0.15
Hue adjustment max intensity	0.05	0.10
Gaussian blurring probability	0	0.20
ClassMix [29] probability	0.20	0.80

Table 2. Performance (Mean IoU) for the Cityscapes *val* set for different labeled-unlabeled ratios and, in parentheses, the difference w.r.t. the corresponding fully supervised (FS) result.

method	1/30	1/8	1/4	FS
<i>Architecture: Deeplabv2 with ResNet-101 backbone</i>				
Adversarial [19]+	—	58.8 (-7.6)	62.3 (-4.1)	66.4
s4GAN [27]*	—	59.3 (-6.7)	61.9 (-4.9)	66.0
French <i>et al.</i> [13]*	51.2 (-16.3)	60.3 (-7.2)	63.9 (-3.6)	67.5
CBC [11]+	48.7 (-18.2)	60.5 (-6.4)	64.4 (-2.5)	66.9
ClassMix [29]+	54.1 (-12.1)	61.4 (-4.8)	63.6 (-2.6)	66.2
DMT [12]*+	54.8 (-13.4)	63.0 (-5.2)	—	68.2
Ours*	58.0 (-8.4)	63.0 (-3.4)	64.8 (-1.6)	66.4
Ours+	59.4 (-7.9)	64.4 (-2.9)	65.9 (-1.4)	67.3

Architecture: Deeplabv3+ with ResNet-50 backbone

Error-corr [26]*	—	67.4 (-7.4)	70.7 (-4.1)	74.8
Ours*	64.9 (-9.3)	70.0 (-4.2)	71.6 (-2.6)	74.2

* ImageNet pre-training, + COCO pre-training

Table 3. Performance (Mean IoU) for the Pascal VOC *val* set for different labeled-unlabeled ratios and, in parentheses, the difference w.r.t. the corresponding fully supervised (FS) result.

method	1/50	1/20	1/8	FS
<i>Architecture: Deeplabv2 with ResNet-101 backbone</i>				
Adversarial [19]+	57.2 (-17.7)	64.7 (-10.2)	69.5 (-5.4)	74.9
s4GAN [27]+	63.3 (-10.3)	67.2 (-6.4)	71.4 (-2.2)	73.6
French <i>et al.</i> [13]*	64.8 (-7.7)	66.5 (-6.0)	67.6 (-4.9)	72.5
CBC [11]+	65.5 (-8.1)	69.3 (-4.3)	70.7 (-2.9)	73.6
ClassMix [29]+	66.2 (-7.9)	67.8 (-6.3)	71.0 (-3.1)	74.1
DMT [12]*+	67.2 (-7.6)	69.9 (-4.9)	72.7 (-2.1)	74.8
Ours*	65.4 (-7.2)	67.8 (-5.1)	69.9 (-2.7)	72.6
Ours+	67.9 (-6.2)	70.0 (-4.1)	71.6 (-2.5)	74.1

Architecture: Deeplabv3+ with ResNet-50 backbone

Error-corr [26]*	—	—	70.2 (-6.1)	76.3
Ours*	63.4 (-12.5)	69.1 (-6.8)	71.8 (-4.1)	75.9

* ImageNet pre-training, + COCO pre-training

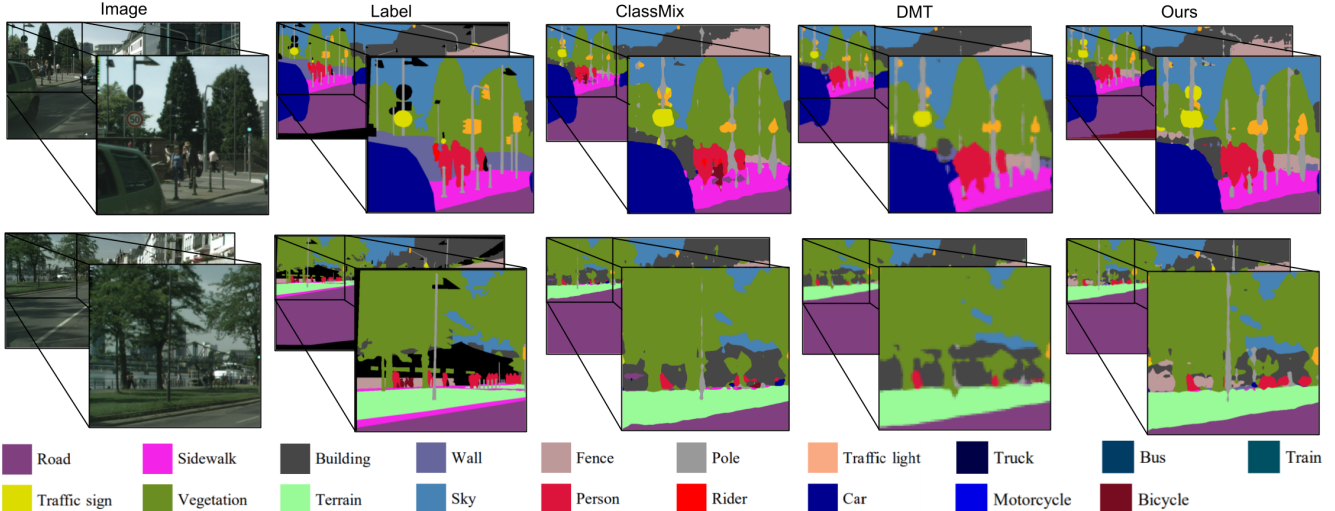


Figure 4. Qualitative results on Cityscapes. Models are trained with $\frac{1}{8}$ of the labeled data using Deeplabv2 with ResNet-101. From left to right: Image, manual annotations, ClassMix [29], DMT [12], our approach.

4.3.1 Semi-supervised Semantic Segmentation

Cityscapes. Table 2 compares different methods on the Cityscapes benchmark for different labeled-unlabeled rates: $\frac{1}{30}$, $\frac{1}{8}$ and, $\frac{1}{4}$. Fully Supervised (FS) scenario, where all images are labeled, is also shown as a reference. As shown in the table, our approach outperforms the current state-of-the-art by a significant margin in all settings. The performance difference is increasing as less labeled data is available, demonstrating the effectiveness of our approach. This is particularly important since the goal of semi-supervised learning is to learn with as little supervision as possible. Note that the upper bound for each method is shown in the fully supervised setting (FS).

Figure 4 shows a visual comparison of the top-performing methods on different relevant samples from Cityscapes. Note in these examples how our approach improves on fine-grained examples (e.g., poles, traffic lights, signs, or people).

Pascal VOC. Table 3 shows the comparison of different methods on the Pascal VOC benchmark, using different labeled-unlabeled rates: $\frac{1}{50}$, $\frac{1}{20}$ and, $\frac{1}{8}$. Our proposed method outperforms previous methods for most of the configurations. Like in the previous benchmark, our method presents larger benefits for the more challenging cases, *i.e.*, only a small fraction of data is labeled ($\frac{1}{50}$). This demonstrates that the proposed approach is especially effective to learn from unlabeled data.

4.3.2 Semi-supervised Domain Adaptation

Semi-supervised domain adaptation for semantic segmentation differs from the semi-supervised set-up in the avail-

ability of labeled data from another domain. That is, apart from having $\mathcal{X}_l = \{x_l, y_l\}$ and $\mathcal{X}_u = \{x_u\}$ from the target domain, a large set of labeled data from another domain is also available: $\mathcal{X}_d = \{x_d, y_d\}$.

Our method can naturally tackle this task by evenly sampling from both \mathcal{X}_l and \mathcal{X}_d as our labeled data when optimizing \mathcal{L}_{sup} and $\mathcal{L}_{\text{contr}}$. However, the memory bank only stores features from the target domain \mathcal{X}_l . In this way, both the features from unlabeled data \mathcal{X}_u , and the features from the other domain \mathcal{X}_d are aligned with those from \mathcal{X}_l .

Following ASS [42], we take the GTA5 dataset as \mathcal{X}_d , where all elements are labeled, and the Cityscapes is the target domain consisting of a small set of labeled data \mathcal{X}_l and a large set of unlabeled samples \mathcal{X}_u . Table 4 compares the results of our method with ASS, state-of-the-art on this task, both using ImageNet pre-training for a fair comparison. For reference, we also show the results of our approach with no adaptation, *i.e.*, only training on the target domain Cityscapes, as we do for the semi-supervised set up from the previous experiment (Table 2). We can see that

Table 4. Mean IoU in Cityscapes *val* set. Central columns evaluate the semi-supervised domain adaptation task (GTA5 \rightarrow Cityscapes). The last column evaluates a semi-supervised setting in Cityscapes (no adaptation). Different labeled-unlabeled ratios for Cityscapes are compared. All methods use ImageNet pre-trained Deeplabv2 with ResNet-101 backbone.

City Labels	ASS [42] with domain adaptation	Ours with domain adaptation	Ours no adaptation
1/30	54.2	59.9	58.0
1/15	56.0	62.0	59.9
1/6	60.2	64.2	63.7
1/3	64.5	65.6	65.1

Table 5. Ablation study on the different losses included (Equation 1). Mean IoU obtained on Cityscapes benchmark ($\frac{1}{30}$ available labels, Deeplabv2-ResNet101 COCO pre-trained).

\mathcal{L}_{sup}	$\mathcal{L}_{\text{pseudo}}$	\mathcal{L}_{ent}	$\mathcal{L}_{\text{contr}}$	mIoU
✓				49.5
✓	✓			56.7
✓		✓		52.2
✓			✓	54.4
✓	✓	✓		57.4
✓	✓		✓	59.0
✓		✓	✓	57.3
✓	✓	✓	✓	59.4

our approach benefits from the use of the other domain data (GTA5), especially where there is little labeled data available ($\frac{1}{30}$), as it could be expected. Our method outperforms ASS by a large margin in all the different set-ups. As in previous experiments, our improvement is more significant when the amount of available labeled data is smaller.

4.4. Ablation Experiments

The following experiments study the impact of the different components of the proposed approach. The evaluation is done on the Cityscapes data, since it provides more complex scenes compared to Pascal VOC. We select the challenging labeled data ratio of $\frac{1}{30}$.

Losses impact. Table 5 shows the impact of every loss used by the proposed method. We can observe that the four losses are complementary, getting a 10 mIoU increase over our baseline model, using only the supervised training when $\frac{1}{30}$ of the Cityscapes labeled data is available. Note that our proposed contrastive module $\mathcal{L}_{\text{contr}}$ is able to get 54.32 mIoU even without any other complementary loss, which is the previous state-of-the-art for this set-up (see Table 2). Adding the $\mathcal{L}_{\text{pseudo}}$ significantly improves the performance and then, adding \mathcal{L}_{ent} regularization loss gives a little extra performance gain.

Contrastive module. Table 6 shows an ablation on the influence of the contrastive module for different values of λ_{contr} (Equation 1). As expected, if this value is too low, the effect gets diluted, with similar performance as if the proposed loss is not used at all (see Table 5). High values are also detrimental, probably because it acts as increasing the learning rate vastly, which hinders the optimization. The best performance is achieved when this contrastive loss acts as auxiliary ($\lambda_{\text{contr}} = 10^{-1}$), i.e., its weight is a little lower than the segmentation losses (\mathcal{L}_{sup} and $\mathcal{L}_{\text{pseudo}}$).

The effect of the size (per-class) of our memory bank is studied in Table 7. As expected, higher values lead

Table 6. Effect of different values for the factor λ_{contr} (Equation 1) that weights the effect of the contrastive loss $\mathcal{L}_{\text{contr}}$. Results on Cityscapes benchmark ($\frac{1}{30}$ available labels, Deeplabv2-ResNet101 COCO pre-trained).

λ_{contr}	10^4	10^2	10^1	10^0	10^{-1}	10^{-2}	10^{-4}
mIoU	50.3	51.4	54.8	59.1	59.4	58.7	57.6

Table 7. Effect of our contrastive learning memory bank size (features per-class), ψ . Results on Cityscapes benchmark ($\frac{1}{30}$ available labels, Deeplabv2-ResNet101 COCO pre-trained).

ψ	32	64	128	256	512
mIoU	58.7	58.9	59.2	59.4	59.3

Table 8. Ablation study of our contrastive module main components. Results on Cityscapes benchmark ($\frac{1}{30}$ available labels, using Deeplabv2-ResNet101 COCO pre-trained).

Base	f_{ξ}	$S_{c,\theta}$	FQF	mIoU
✓				58.3
✓	✓			58.7
✓		✓		58.6
✓			✓	59.0
✓	✓	✓	✓	59.4

f_{ξ} : Use teacher model f_{ξ} to extract features instead of f_{θ}
 $S_{c,\theta}$: Use class-specific attention $S_{c,\theta}$ to weight every feature
 FQF: Feature Quality Filter for Memory Bank update

to stronger performances, although from 256 up they tend to maintain similarly. Because all the elements from the memory bank are used during the contrastive optimization (Equation 11) the larger the memory bank is, the more computation and memory it requires. Therefore, we select 256 as our default value.

Table 8 studies the effect of the main components used in the proposed contrastive learning module. The base configuration of the module still presents a performance gain compared to not using the contrastive module. This shows that our simplest implementation of the per-pixel contrastive learning using the memory bank already helps to improve the segmentation task in a semi-supervised scenario. Generating and selecting good quality prototypes is the most important factor. This is done both by the Feature Quality Filter (FQF), i.e., checking that the feature leads to an accurate and confident prediction, and extracting them with the teacher network f_{ξ} . Then, using the class-specific attention $S_{c,\theta}$ to weight every sample (both from the memory bank and input sample) is also beneficial, acting as a learned sampling method.

5. Conclusion

This paper presents a novel approach for semi-supervised semantic segmentation. Our work shows the benefits of incorporating contrastive learning techniques to solve this semi-supervised task. The proposed contrastive learning module boosts the performance of semantic segmentation in these settings. Our new module contains a memory bank that is continuously updated with selected features from those produced by a teacher network from labeled data. These features are selected based on their quality and relevance for the contrastive learning. Our student network is optimized for both labeled and unlabeled data to learn similar class-wise features to those in the memory bank. The use of contrastive learning at a pixel-level has been barely exploited and this work demonstrates the potential and benefits it brings to semi-supervised semantic segmentation and semi-supervised domain adaptation. Our results outperform state-of-the-art on several public benchmarks, with particularly significant improvements on the more challenging set-ups, *i.e.*, when the amount of available labeled data is low.

References

- [1] Iñigo Alonso, Luis Riazuelo, and Ana C Murillo. Mininet: An efficient semantic segmentation convnet for real-time robotic applications. *IEEE Transactions on Robotics (T-RO)*, 2020. [1](#)
- [2] Vijay Badrinarayanan, Alex Kendall, and Roberto Cipolla. Segnet: A deep convolutional encoder-decoder architecture for image segmentation. *IEEE Transactions on Pattern Analysis and Machine Intelligence*, 39(12):2481–2495, 2017. [1](#)
- [3] David Berthelot, Nicholas Carlini, Ian Goodfellow, Nicolas Papernot, Avital Oliver, and Colin A Raffel. Mixmatch: A holistic approach to semi-supervised learning. In *Advances in Neural Information Processing Systems*, pages 5049–5059, 2019. [2](#)
- [4] Liang-Chieh Chen, George Papandreou, Iasonas Kokkinos, Kevin Murphy, and Alan L Yuille. Deeplab: Semantic image segmentation with deep convolutional nets, atrous convolution, and fully connected crfs. *IEEE transactions on pattern analysis and machine intelligence*, 40(4):834–848, 2017. [5](#)
- [5] Ting Chen, Simon Kornblith, Mohammad Norouzi, and Geoffrey Hinton. A simple framework for contrastive learning of visual representations. *arXiv preprint arXiv:2002.05709*, 2020. [2](#)
- [6] Xinlei Chen, Haoqi Fan, Ross Girshick, and Kaiming He. Improved baselines with momentum contrastive learning. *arXiv preprint arXiv:2003.04297*, 2020. [2](#)
- [7] Xinlei Chen and Kaiming He. Exploring simple siamese representation learning. *arXiv preprint arXiv:2011.10566*, 2020. [2](#)
- [8] Marius Cordts, Mohamed Omran, Sebastian Ramos, Timo Rehfeld, Markus Enzweiler, Rodrigo Benenson, Uwe Franke, Stefan Roth, and Bernt Schiele. The cityscapes dataset for semantic urban scene understanding. In *Proceedings of IEEE Conference on CVPR*, pages 3213–3223, 2016. [5](#)
- [9] Terrance DeVries and Graham W Taylor. Improved regularization of convolutional neural networks with cutout. *arXiv preprint arXiv:1708.04552*, 2017. [3](#)
- [10] Mark Everingham, Luc Van Gool, Christopher KI Williams, John Winn, and Andrew Zisserman. The pascal visual object classes (voc) challenge. *International journal of computer vision*, 88(2):303–338, 2010. [5](#)
- [11] Zhengyang Feng, Qianyu Zhou, Guangliang Cheng, Xin Tan, Jianping Shi, and Lizhuang Ma. Semi-supervised semantic segmentation via dynamic self-training and class-balanced curriculum. *arXiv preprint arXiv:2004.08514*, 2020. [2](#), [3](#), [5](#), [6](#)
- [12] Zhengyang Feng, Qianyu Zhou, Qiqi Gu, Xin Tan, Guangliang Cheng, Xuequan Lu, Jianping Shi, and Lizhuang Ma. Dmt: Dynamic mutual training for semi-supervised learning. *arXiv preprint arXiv:2004.08514*, 2020. [3](#), [6](#), [7](#)
- [13] Geoff French, Samuli Laine, Timo Aila, and Michal Mackiewicz. Semi-supervised semantic segmentation needs strong, varied perturbations. In *29th British Machine Vision Conference, BMVC 2020*, 2019. [1](#), [3](#), [6](#)
- [14] Ian Goodfellow, Jean Pouget-Abadie, Mehdi Mirza, Bing Xu, David Warde-Farley, Sherjil Ozair, Aaron Courville, and Yoshua Bengio. Generative adversarial nets. *Advances in neural information processing systems*, 27:2672–2680, 2014. [3](#)
- [15] Yves Grandvalet and Yoshua Bengio. Semi-supervised learning by entropy minimization. *Advances in neural information processing systems*, 17:529–536, 2004. [2](#)
- [16] Jean-Bastien Grill, Florian Strub, Florent Altché, Corentin Tallec, Pierre H Richemond, Elena Buchatskaya, Carl Dohersch, Bernardo Avila Pires, Zhaohan Daniel Guo, Mohammad Gheshlaghi Azar, et al. Bootstrap your own latent: A new approach to self-supervised learning. *arXiv preprint arXiv:2006.07733*, 2020. [2](#), [4](#), [5](#)
- [17] Raia Hadsell, Sumit Chopra, and Yann LeCun. Dimensionality reduction by learning an invariant mapping. In *2006 IEEE Computer Society Conference on Computer Vision and Pattern Recognition (CVPR'06)*, volume 2, pages 1735–1742. IEEE, 2006. [2](#)
- [18] Lang Huang, Chao Zhang, and Hongyang Zhang. Self-adaptive training: Bridging the supervised and self-supervised learning. *arXiv preprint arXiv:2101.08732*, 2021. [2](#)
- [19] Wei-Chih Hung, Yi-Hsuan Tsai, Yan-Ting Liou, Yen-Yu Lin, and Ming-Hsuan Yang. Adversarial learning for semi-supervised semantic segmentation. *arXiv preprint arXiv:1802.07934*, 2018. [1](#), [3](#), [5](#), [6](#)
- [20] Sergey Ioffe and Christian Szegedy. Batch normalization: Accelerating deep network training by reducing internal covariate shift. *arXiv preprint arXiv:1502.03167*, 2015. [5](#)
- [21] Simon Jégou, Michal Drozdal, David Vazquez, Adriana Romero, and Yoshua Bengio. The one hundred layers tiramisu: Fully convolutional densenets for semantic segmentation. In *CVPR Workshops*. IEEE, 2017. [1](#)

- [22] Tarun Kalluri, Girish Varma, Manmohan Chandraker, and CV Jawahar. Universal semi-supervised semantic segmentation. In *Proceedings of the IEEE International Conference on Computer Vision*, pages 5259–5270, 2019. 2
- [23] Dong-Hyun Lee. Pseudo-label: The simple and efficient semi-supervised learning method for deep neural networks. In *Workshop on challenges in representation learning, ICML*, volume 3, 2013. 1, 2
- [24] Andrew L Maas, Awni Y Hannun, and Andrew Y Ng. Rectifier nonlinearities improve neural network acoustic models. In *Proceedings icml*, volume 30, page 3, 2013. 5
- [25] Geoffrey J McLachlan. Iterative reclassification procedure for constructing an asymptotically optimal rule of allocation in discriminant analysis. *Journal of the American Statistical Association*, 70(350):365–369, 1975. 2
- [26] Robert Mendel, Luis Antonio de Souza, David Rauber, João Paulo Papa, and Christoph Palm. Semi-supervised segmentation based on error-correcting supervision. In *European Conference on Computer Vision*, pages 141–157. Springer, 2020. 5, 6
- [27] Sudhanshu Mittal, Maxim Tatarchenko, and Thomas Brox. Semi-supervised semantic segmentation with high-and low-level consistency. *IEEE Transactions on Pattern Analysis and Machine Intelligence*, 2019. 1, 3, 5, 6
- [28] Vinod Nair and Geoffrey E Hinton. Rectified linear units improve restricted boltzmann machines. In *ICML*, 2010. 5
- [29] Viktor Olsson, Wilhelm Traneheden, Juliano Pinto, and Lennart Svensson. Classmix: Segmentation-based data augmentation for semi-supervised learning. In *Proceedings of the IEEE/CVF Winter Conference on Applications of Computer Vision*, pages 1369–1378, 2021. 1, 2, 3, 5, 6, 7
- [30] Stephan R Richter, Vibhav Vineet, Stefan Roth, and Vladlen Koltun. Playing for data: Ground truth from computer games. In *European conference on computer vision*, pages 102–118. Springer, 2016. 5
- [31] Olaf Ronneberger, Philipp Fischer, and Thomas Brox. U-net: Convolutional networks for biomedical image segmentation. In *International Conference on Medical image computing and computer-assisted intervention*, pages 234–241. Springer, 2015. 1
- [32] Mehdi Sajjadi, Mehran Javanmardi, and Tolga Tasdizen. Regularization with stochastic transformations and perturbations for deep semi-supervised learning. In *Advances in neural information processing systems*, pages 1163–1171, 2016. 2
- [33] H Scudder. Probability of error of some adaptive pattern-recognition machines. *IEEE Transactions on Information Theory*, 11(3):363–371, 1965. 2
- [34] Kihyuk Sohn, David Berthelot, Chun-Liang Li, Zizhao Zhang, Nicholas Carlini, Ekin D Cubuk, Alex Kurakin, Han Zhang, and Colin Raffel. Fixmatch: Simplifying semi-supervised learning with consistency and confidence. *arXiv preprint arXiv:2001.07685*, 2020. 2, 4
- [35] Shuyang Sun, Liang Chen, Gregory Slabaugh, and Philip Torr. Learning to sample the most useful training patches from images. *arXiv preprint arXiv:2011.12097*, 2020. 5
- [36] Antti Tarvainen and Harri Valpola. Weight-averaged consistency targets improve semi-supervised deep learning results. 2, 3
- [37] Antti Tarvainen and Harri Valpola. Mean teachers are better role models: Weight-averaged consistency targets improve semi-supervised deep learning results. In *Advances in neural information processing systems*, pages 1195–1204, 2017. 1, 2, 3, 5
- [38] Jesper E Van Engelen and Holger H Hoos. A survey on semi-supervised learning. *Machine Learning*, 109(2):373–440, 2020. 1
- [39] Wouter Van Gansbeke, Simon Vandenhende, Stamatis Georgoulis, and Luc Van Gool. Unsupervised semantic segmentation by contrasting object mask proposals. *arXiv preprint arXiv:2102.06191*, 2021. 2
- [40] Wenguan Wang, Tianfei Zhou, Fisher Yu, Jifeng Dai, Ender Konukoglu, and Luc Van Gool. Exploring cross-image pixel contrast for semantic segmentation. *arXiv preprint arXiv:2101.11939*, 2021. 2
- [41] Xinlong Wang, Rufeng Zhang, Chunhua Shen, Tao Kong, and Lei Li. Dense contrastive learning for self-supervised visual pre-training. *arXiv preprint arXiv:2011.09157*, 2020. 2
- [42] Zhonghao Wang, Yunchao Wei, Rogerio Feris, Jinjun Xiong, Wen-Mei Hwu, Thomas S Huang, and Honghui Shi. Alleviating semantic-level shift: A semi-supervised domain adaptation method for semantic segmentation. In *Proceedings of the IEEE/CVF Conference on Computer Vision and Pattern Recognition Workshops*, pages 936–937, 2020. 5, 7
- [43] Zhirong Wu, Yuanjun Xiong, Stella X Yu, and Dahua Lin. Unsupervised feature learning via non-parametric instance discrimination. In *Proceedings of the IEEE Conference on Computer Vision and Pattern Recognition*, pages 3733–3742, 2018. 2
- [44] Saining Xie, Jiatao Gu, Demi Guo, Charles R Qi, Leonidas Guibas, and Or Litany. Pointcontrast: Unsupervised pre-training for 3d point cloud understanding. In *European Conference on Computer Vision*, pages 574–591. Springer, 2020. 2
- [45] Zhenda Xie, Yutong Lin, Zheng Zhang, Yue Cao, Stephen Lin, and Han Hu. Propagate yourself: Exploring pixel-level consistency for unsupervised visual representation learning. *arXiv preprint arXiv:2011.10043*, 2020. 2
- [46] Mang Ye, Xu Zhang, Pong C Yuen, and Shih-Fu Chang. Unsupervised embedding learning via invariant and spreading instance feature. In *Proceedings of the IEEE Conference on computer vision and pattern recognition*, pages 6210–6219, 2019. 2
- [47] Sangdoo Yun, Dongyoon Han, Seong Joon Oh, Sanghyuk Chun, Junsuk Choe, and Youngjoon Yoo. Cutmix: Regularization strategy to train strong classifiers with localizable features. In *Proceedings of the IEEE/CVF International Conference on Computer Vision*, pages 6023–6032, 2019. 3